Indian Journal of Biochemistry & Biophysics
Vol. 58, February 2021, pp. 62-70

Evaluation of antiproliferative potential of manganese (II)-dafone complex

Reena[1], Biju AR[2]*, Megha P Nambiar[2] & Bonige Kishore Babu[3]

[1]Department of Chemistry, Pazhassi Raja N.S.S. College, Mattanur-670 702, Kerala, India

[2]Department of Chemistry, Sir Syed College, Taliparamba-670142, Kerala, India

[3]Department of Engineering Chemistry, Andhra University College of Engineering (A), Visakhapatnam-530 003, Andhra Pradesh, India

Received 06 November 2020; *revised 27 January 2021*

Cytotoxicity is the quality of being toxic to cells. *In vitro* toxicity is the scientific analysis of the effect of toxic chemical substances on cultured bacteria or mammalian cells. In our work Manganese–4,5-Diazafluoren-9-one complex was prepared and its cytotoxicity was studied by standard MTT Assay in Cervical carcinoma cells HeLa. The result was compared with the normal fibroblast cell to check its influence on normal cells. On comparing the results, the complex is found to be more toxic to cervical carcinoma cells than the normal fibroblast cells. The photocatalytic activity of the complex was studied on the basis of the decomposition reaction of methylene blue dye in presence of the complex. The compound $[Mn(C_{11}H_6N_2O)_2(NCS)_2]$ was synthesised and characterised by various spectroscopic methods and the structure was confirmed by single– crystal XRD analysis. The molecular structure of the complex was optimized using density functional theory (DFT) at the B3LYP/6–311 G (d,p) level. The smallest HOMO–LUMO energy gap (0.66 eV) indicates the soft acid nature of the complex.

Keywords: Crystal structure, Cytotoxicity, DFT studies, 4,5-Diazafluoren-9-one, Photocatalyst

Cancer, also called malignancy, is an abnormal growth of cells. There are five types of cancer known as carcinoma, lymphoma, melanoma, sarcoma, and leukemia. Carcinoma is the most commonly diagnosed cancer, originate in the skin, lungs, breasts, pancreas, and other organs and glands. In cervical carcinoma lowermost part of the uterus (cervix) was affected. It is the fourth most common cancer in women. According to WHO, in 2018, approximately 5,70,000 women were diagnosed with cervical cancer worldwide and about 3,11,000 women died from the disease.

Dafone is a bidentate ligand similar to 1,10-phenanthroline and bipyridine. It is a derivative of 1,10-phenanthroline, having an exocyclic keto group[1,2], which make it suitable for further derivatisation, to yield multinuclear metal complexes having interesting catalytic and biological properties[3]. Metal coordination complexes have been widely studied for their anticancer activities[4-9]. Earlier platinum– based complexes like cisplatin and carboplatin were used for the treatment of various cancers. In spite of their effectiveness, they lack selectivity for tumour tissues, which leads to severe side effects like neurotoxicity and ototoxicity. Moreover, some tumor cell lines are now growing resistant to cisplatin. So researchers are trying to synthesize new compounds that are selectively toxic to tumor cells[10,11] and cause no harm to normal cells. Titanium complex titanocene dichloride was clinically approved for its higher cytotoxicity in renal cell carcinoma[12] and human ovarian cancer[13]. Recent studies support the cytotoxicity of phenanthroline derivative against various cell lines including cisplatin– resistant cell lines[14,15]. A cisplatin analogue cis-Pt(dafone)Cl_2 shows considerable cytotoxicity against HeLa and Hacat cell lines[16]. Silver complexes have been reported to have anticancer activity. Silver carboxylate dimers possess anticancer activity against human carcinoma cells[17] and silver phosphine complexes are active against cisplatin– resistant cell lines[18]. Several Cu (II) chelates have been reported to exhibit enhanced antiproliferative activity[19,20]. On analysing these results we decided to find out the cytotoxic character of the title complex.

A photocatalyst is a material that absorbs light to bring it to a higher energy level and provides such energy to a reacting substance to make a chemical reaction occur. Environmental pollution gets more and

*Correspondence:
E-mail: biju@sirsyedcollege.ac.in

Abbreviations: dafone, 4,5diazafluoren-9-one; DFT, density functional theory; FMO, Frontier Molecular Orbitals; LC_{50}, Lethel concentration[50]

more public concern in our society[21,22]. Wastewater containing dyes coming from textile and paper industry is generally high in both color and organic content[23]. Therefore, decolourization process were important in waste water treatment. Decontamination of polluted water by photocatalysis was low cost and effective[24]. A lot of work has been done to develop heterogeneous photocatalyst with high photocatalytic activities for environmental applications such as water disinfection, hazardous waste remediation, and water purification[25-27].

Even though the DNA interaction properties[28-30] of dafone attracted the attention of many researchers, the co-ordination chemistry of dafone is still restricted to a few metals[31-34]. There is only one report[35] for Mn(II) dafone coordination complex $[Mn(dafone)_2Cl_2]$, in which dafone coordinates to Mn(II) in *cis*-mode. There is also report of crystallography of Co(II) $[Co(dafone)_2(NCS)_2]$[36], Zn(II) $[Zn(dafone)_2I_2]$[37], Cu(II) $[Cu(dafone)_2(SCN)_2]$[38] and $[Cu(dafone)_2(NCO)_2]$ MeCN[35], Ni(II) $[Ni(dafone)_2(SCN)_2]$[38] and $[Ni(dafone)_2(NCS)_2]$[39] and Hg(II) $[Hg(dafone)(SCN)_2]$[38] complexes. In both cobalt and zinc complexes, dafone coordinates in *cis*-mode. The crystallography of the title compound was analysed by various spectroscopic methods and confirmed by single –crystal XRD studies.

Our research work was conducted to find out the cytotoxicity of Manganese – 4,5-Diazafluoren-9-one Complex by standard MTT Assay in Cervical carcinoma cells HeLa (an immortal cell line derived from cervical cancer cells). Selectivity for tumour tissue was checked by its action on Fibroblast cells (L929) (a type of biological cell that synthesises the extracellular matrix and collagen and the most common connective tissue in animals). A compound that is toxic to HeLa cell lines and non-toxic to fibroblast cell lines will be safe for cancer treatment. The photocatalytic activity of the prepared complex was carried out based on degradation of methylene blue dye in presence of the complex using a UV lamp as the source of radiation. The crystallography of the Manganese – 4,5-Diazafluoren-9-one complex was analysed by various spectroscopic methods and confirmed by single– crystal XRD studies.

Materials and Methods

All chemicals were purchased from Ranbaxy chemicals and Sigma Aldrich and used without further purification. Dafone was prepared as per the reported procedure[1]. It was precipitated as yellow–orange needles within 1-2 days. IR spectra were measured by using the Thermo Nicolet AVATAR model FTIR spectrometer using the KBr pellets. An elemental analysis experiment was conducted from SAIF STIC Cochin, Kerala, India.

Synthesis of $[Mn(dafone)_2(NCS)_2]$

Manganese perchlorate (0.3619 g, 1 mmol) and Ammonium Thiocyanate (0.152 g, 2.00 mmol) were dissolved in a minimum amount of water. To this solution, dafone (0.364 g, 2.00 mmol) dissolved in a minimum amount of acetonitrile was added slowly and kept undisturbed. Golden yellow shining needles were formed within ten days. Yield 0.4113 g (76.81 mmol, 76.81%). Anal (%) Calcd. for $C_{24}H_{12}MnN_6O_2S_2$: C, 53.78; H, 2.24; N, 15.69; S, 11.97. Found: C, 54.05; H, 1.32; N, 16.36; S, 11.24; IR (KBr, cm^{-1}) 3431, 3088, 2067, 2053, 1735, 1570, 1412, 1248, 1101, 755 and 524. The crystals are stable in air and melt above 280°C.

Cytotoxic Study

Cytotoxicity of the complex was conducted from Biogenix Research Centre, Thiruvananthapuram, Kerala, India using cervical carcinoma cells (HeLa) and compare the result obtained with normal fibroblast cells (L929). Viability of the cell was evaluated by direct observation of cells by inverted phase– contrast microscope followed by MTT assay method. Any detectable changes in the morphology of the cells, such as rounding or shrinking of cells, granulation, and vacuolization in the cytoplasm of the cells were considered as indicators of cytotoxicity.

Photocatalytic activity

Photocatalytic activity of the prepared complex was carried out using methylene blue dye as the pollutant and UV lamp as the source of radiation. The metal complex (0.01 g) and an aqueous solution of methylene blue (70 mL) were mixed in a beaker and were equilibrated by constant stirring at room temperature in dark for 30 min to allow the adsorption of methylene blue dye, if any, by the complex. The solution is stirred under UV light. The sample was allowed to absorb UV light and 5 mL aliquots were taken and filtered at a definite time interval of 30 min. The filtrate was analysed using a UV-Visible spectrophotometer. When the reaction mixture was stirred, the complex absorbs UV rays and get excited due to the appropriate bandgap. The photogenerated electron– hole pairs produce hydroxyl radicals in the system which decolorises the blue–colored methylene blue solution[38,39]. The intensity of absorption peak of methylene blue at 663 nM gets diminished gradually

with the extension of the exposure time indicating the degradation of methylene blue dye[40-41].

X-Ray Crystallography

X-ray diffraction data were collected on a Bruker Kappa APEX2 CCD diffractometer, equipped with graphite monochromated Mo Kα radiation (λ = 0.71073Å) at 298 K. Datas were reduced using Computer programs: *APEX2*[42], SIR92[43], *S*HELXL2014/7[44], Mercury[45], publCIF[46]. The analysis was carried out from SAIF STIC, Kochin.

Computational Analysis

The highest occupied molecular orbital (HOMO) and lowest unoccupied molecular orbital (LUMO) are called Frontier Molecular Orbitals (FMO). The molecular structure of the complex was optimized using density functional theory (DFT). DFT calculations were performed for the complex $[Mn(dafone)_2(NCS)_2]$ with computational program Guassian09[47] using the basis set B3LYP/6–311 G(d,p)[48].

Results and Discussion

Characterization of the ligand and the complex

Ligand and complex were characterized by various spectroscopic studies. IR Spectrum of dafone shows three characteristic bands, whose wavelengths corresponding to the stretching vibrations of its three types of bonds: 3304 cm^{-1} (υ_{C-H}), 1714 cm^{-1} ($\upsilon_{C=O}$), and 1461 cm^{-1} ($\upsilon_{C=N}$). In the IR spectrum of the complex, a strong band in 1410 cm^{-1} may be due to azomethine group (C=N) and a broadband in 1740 cm^{-1} may be due to stretching vibrations of C=O group. The absorption band at 590 nM may be assigned to $^6A_{1g} \rightarrow {}^4T_{1g}$ (G) transition indicate the octahedral geometry of the complex $[Mn(dafone)_2 (NCS)_2]$. Molar conductivity of ~10^{-3} M solution of the complex in DMF was found to be 12 Sm^2mol^{-1} at room temperature, indicate the non– electrolytic nature of $[Mn(dafone)_2(NCS)_2]$[49].

Application of the complex $[Mn(dafone)_2(NCS)_2]$

Cytotoxicity

Complex $[Mn(dafone)_2(NCS)_2]$ was tested for anticancer activity against cervical carcinoma cells. The result was compared with the normal fibroblast cell to check its influence on normal cells. Percentage of viability can be calculated by the equation:

$$\text{Percentage viability} = \frac{\text{Mean OD of Samples}}{\text{OD of Control group}} \times 100$$

Percentage viability of $[Mn(dafone)_2(NCS)_2]$ against HeLa cells and Fibroblast cells (Tables 1 & 2) and the corresponding photographs (Figs. 1 & 2) are given. From the graphical comparison (Fig. 3) of the percentage viability of Hela and fibroblast cells against $[Mn(dafone)_2(NCS)_2]$, it is clear that the complex is more toxic to Hela cells than the fibroblast cells in a metal concentration varying from 0-100 µg/mL. The concentration of the complex that can kill 50% of the unwanted cell (LC_{50} Value) was calculated (Table 3) using ED50 PLUS V1.0 Software.

Photocatalytic activity

The photocatalytic activity of the complex was studied based on its degradation reaction with methylene blue dye. On analyzing the absorbance *vs* wavelength graph (Fig. 4) of methylene blue dye, the intensity of the characteristic absorption peak of methylene blue at 663 nM gets diminished gradually with the extension of the exposure time. It is an indication of

Table 1 — Percentage viability of $[Mn(dafone)_2(NCS)_2]$ against HeLa cells

Sample Conc. (µg/mL)	OD value I	OD value II	OD value III	Average OD	% Viability
0	0.4952	0.4896	0.4935	0.4928	100
6.25	0.4015	0.4115	0.4137	0.4089	82.97
12.5	0.3878	0.3892	0.3964	0.3911	79.37
25	0.3620	0.3742	0.3685	0.3682	74.72
50	0.3280	0.3364	0.3295	0.3313	67.23
100	0.2851	0.2973	0.2984	0.2936	59.58

Table 2 — Percentage viability of $[Mn(dafone)_2(NCS)_2]$ against Fibroblast cells

Sample Conc. (µg/mL)	OD value I	OD value II	OD value III	Average OD	% Viability
Control	0.7225	0.7376	0.7282	0.7294	100.00
6.25	0.6988	0.6982	0.6801	0.6924	94.92
12.5	0.6408	0.6319	0.6328	0.6352	87.08
25	0.5532	0.5616	0.5572	0.5573	76.41
50	0.5121	0.5270	0.5206	0.5199	71.28
100	0.4431	0.4574	0.4584	0.4530	62.10

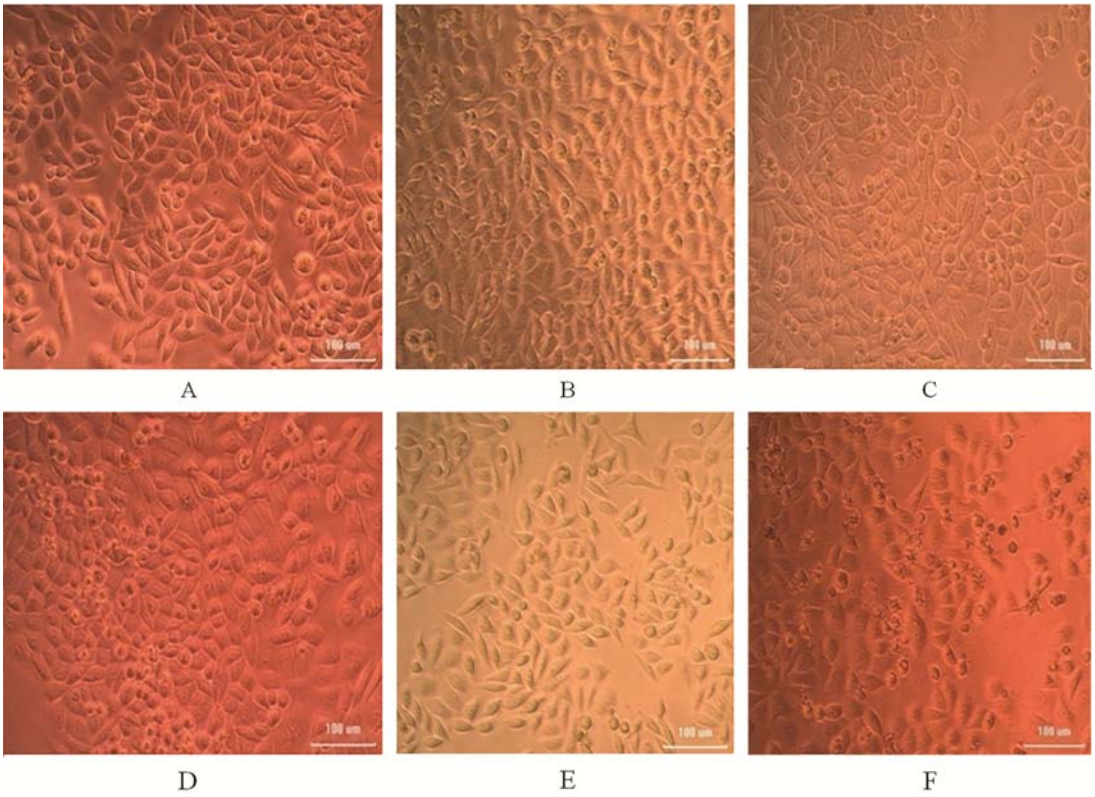

Fig. 1 — Microscopic image of Cervical carcinoma cells (HeLa) when treated with the $[Mn(dafone)_2(NCS)_2]$ in the order of increasing concentration (A) Control; (B) 6.25 µg/mL, (C) 12.5 µg/mL; (D) 25 µg/mL; (E) 50 µg/ mL; and (F) 100 µg/ mL

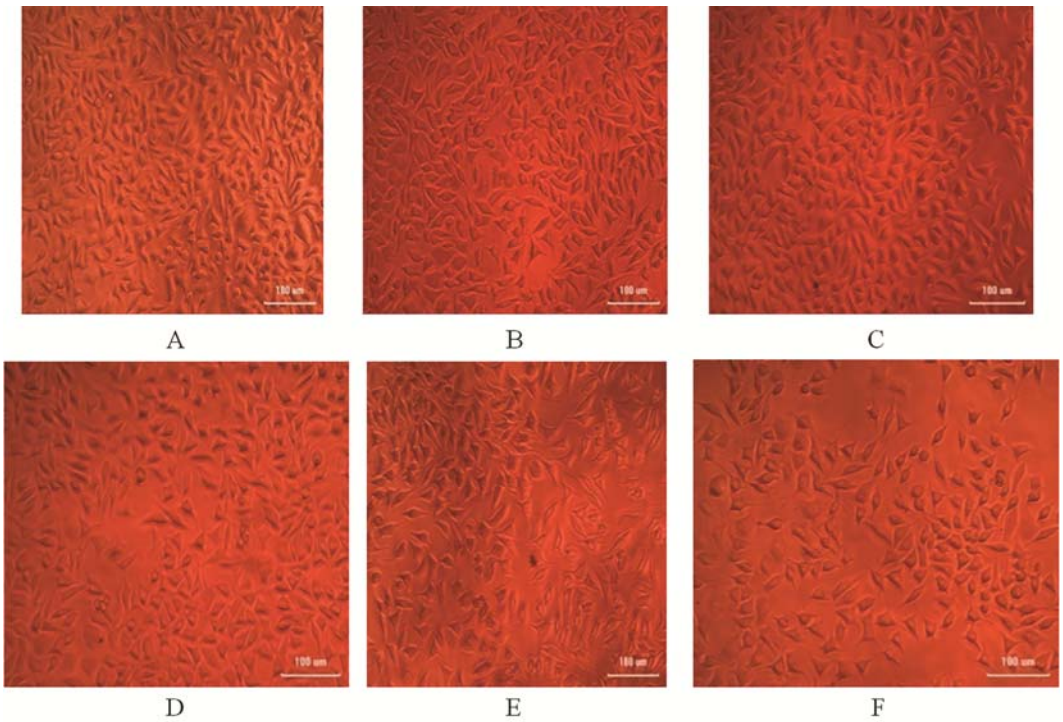

Fig. 2 — Microscopic image of Fibroblast (L929) when treated with the $[Mn(dafone)_2(NCS)_2]$ in the order of increasing concentration (A) Control; (B) 6.25 µg/mL; (C) 12.5 µg/mL; (D) 25 µg/mL; (E) 50 µg/mL; and (F) 100 µg/mL

degradation of methylene blue dye which supports the photocatalytic activity of the complex.

Crystal structure description of [Mn(dafone)$_2$(NCS)$_2$]

Single crystal X-ray diffraction analysis reveal that the complex [Mn(dafone)$_2$(NCS)$_2$] crystallizes in the orthorhombic, P*bcn* with cell parameters *a* =3.3803(10) Å, *b* = 10.4789(7) Å and c= 16.6256(9) Å, α = 90°, *β* =90°, γ = 90° and *Z* = 4 (Fig. 5). Central atom Mn(II) octahedrally coordinated to two thiocyanate anions through nitrogen atoms and two dafone molecules (Fig. 6).

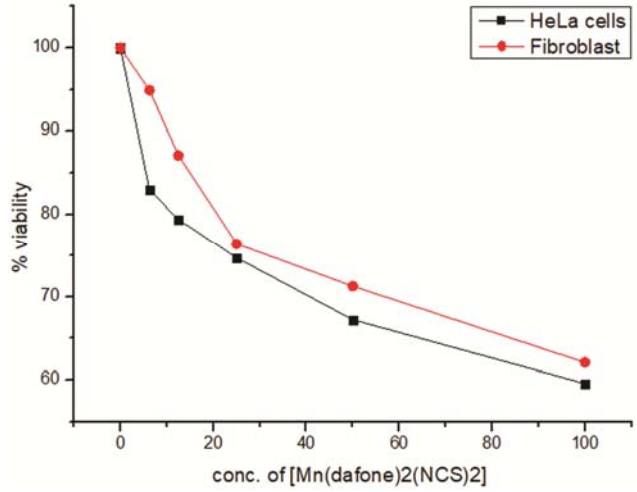

Fig. 3 — A comparison of the percentage viability of Hela and fibroblast cells against the different concentration of [Mn(dafone)$_2$(NCS)$_2$]

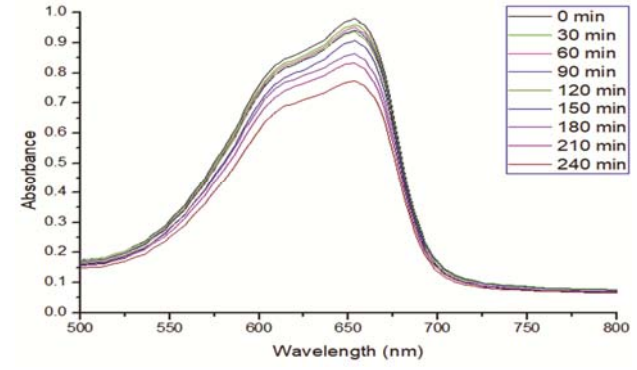

Fig. 4 — Photodegradation plot of methylene blue dye under UV light in presence of [Mn(dafone)$_2$(NCS)$_2$] at various time intervals

Table 3 — LC_{50} Value for the complex [Mn(dafone)$_2$(NCS)$_2$]

Cell lines	Average LC_{50} Value in µg/mL
Cervical carcinoma cells	133.183
Fibroblast cells	129.523

The Mn(II) ions have an octahedral configuration and are located in a special position. Two dafone ligands chelate in cis-mode with an average Mn—N distance of 2.367 Å. The multidentate NCS− ligand coordinates through the nitrogen atom. The Mn—N(NCS) distance is 2.095 Å, which is much shorter than the Mn–dafone distance. The *cis* mode of coordination has been previously observed for both Co(II) and Zn(II) complexes with dafone.

Supramolecular features

The crystal packing of the title compound (Fig. 7) shows several weak intermolecular short contacts and hydrogen bonding interactions, such as C11—H11...N3 (2.721 Å), C11—H11....C12 (2.707 Å), C3—H3....S1 (2.949 Å), C1—H1....C12 (2.870 Å), S1....O1 (3.195 Å) and the contacts expands to become three-dimensional architecture.

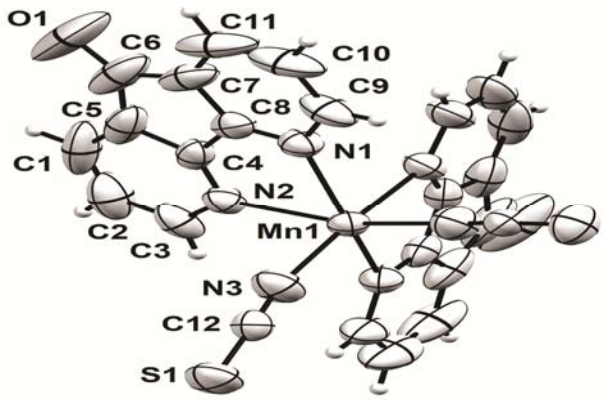

Fig. 5 — The molecular structure of [Mn(dafone)$_2$(NCS)$_2$], with the atom labelling. Displacement ellipsoids are drawn at the 50% probability level

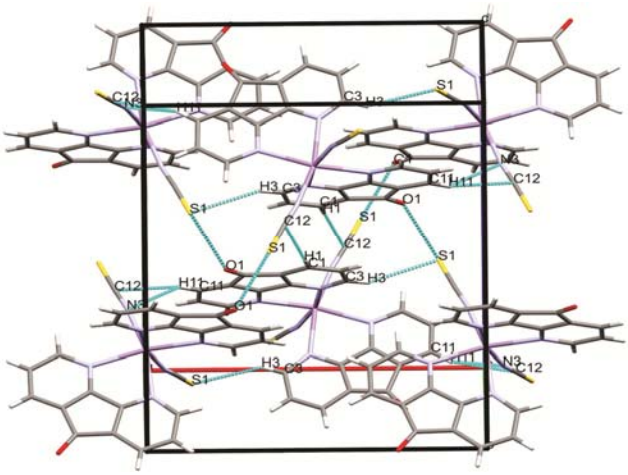

Fig. 6 — A view of the crystal packing of the complex. Dashed lines denote the intermolecular short contact

Refinement

Crystal data, data collection, and structure refinement details (Table 4) are summarized. The C-bound H atoms were positioned geometrically and refined using a riding model, with C—H = 0.93 Å and with *U*iso(H) = 1.2Ueq(C). Selected bond length and bond angles (Table 5) are given.

Frontier Molecular orbital studies

Frontier Molecular Orbitals decides the optoelectronic properties of the molecule. A molecule can be classified into soft and hard acids depending upon the HOMO-LUMO gap. The geometry of the complex is optimised (Fig. 7), and the calculated energy of HOMO and LUMO orbital's of the complex been found to be negative, indicates its stability. The optimized geometry is slightly different from the crystal structure, in which the average Mn1—N2 bond length is increased to 2.64 Å from 2.39 Å and Mn1—N1 and Mn1—N3 distance remains similar 2.32 from 2.34 Å and 2.04 from 2.09 Å, respectively. The HOMO-LUMO gap is calculated to be 0.66 eV, which indicates that the complex molecule is a soft acid. The hardness parameter, which is calculated by the formula of the complex, is

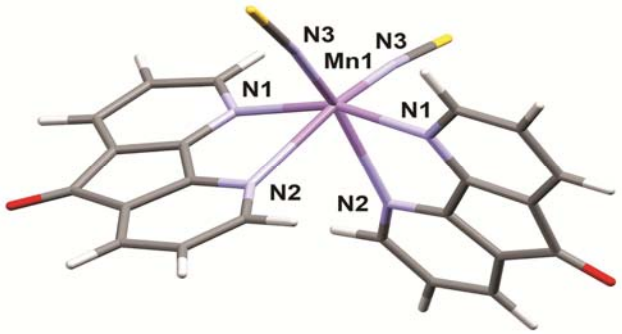

Fig. 7 — Optimized structure of $[Mn(dafone)_2(NCS)_2]$ from computational analysis

Table 4 — Crystal data and structure refinement for $[Mn(dafone)_2(NCS)_2]$

Empirical formula	$C_{24}H_{12}Mn\ N_6O_2S_2$
Formula weight	535.46
Temperature (K)	296(2)
Wavelength(Å)	0.71073
Crystal system	Orthorhombic
Space group	P*bcn*
Unit cell dimensions	
a(Å)	13.3803(10)
b(Å)	10.4789(7)
c(Å)	16.6256(9)
α(°)	90
β(°)	90
γ(°)	90
Volume (Å^3 Å^3)	2331.1(3)
Z	4
D_{calc}(g cm^{-3})	1.526
μ (mm^{-1})	0.781
F (000)	1084
Crystal size (mm)	0.30 x 0.20 x 0.20
Theta range for data collection	2.469 to 28.422 deg.
Limiting indices	17<=h<=17,
Reflections collected / unique	17638 / 2877 [R(int) = 0.0381]
Completeness to theta = 25.242	100.0 %
Absorption correction	Semi empirical from equivalents
Max. and min. transmission	0.859 and 0.800
Refinement method	Full-matrix least-squares on F^2
Data / restraints / parameters	2877 / 0 / 159
Goodness-of-fit	0.919
R_1 [I>2sigma(I)]	0.0470
*wR*2	0.0796
Largest diff. peak and hole	0.413 and -0.293 e.A^{-3}

Table 5 — Selected bond length in [Å] and bond angles in [°] for $[Mn(dafone)_2(NCS)_2]$

Mn1—N3i 2.095 (3)	Mn1—N2i 2.395 (2)
Mn1—N1i 2.338 (2)	
N3—Mn1—N3i 98.51 (15)	N1i—Mn1—N2i 76.02 (8)
N3—Mn1—N1i 107.81 (11)	N1—Mn1—N2i 83.97 (8)
N3i—Mn1—N1i 89.96 (11)	N3—Mn1—N2 165.32 (10)
N3—Mn1—N1 89.96 (11)	N3i—Mn1—N2 90.03 (9)
N3i—Mn1—N1 107.81 (11)	N1i—Mn1—N2 83.97 (8)
N1i—Mn1—N1 152.96 (12)	N1—Mn1—N2 76.02 (8)
N3—Mn1—N2i 90.03 (9)	N2i—Mn1—N2 84.28 (11)
N3i—Mn1—N2i 165.32 (10)	
Symmetry code: (i) −*x*+1, *y*, −*z*+1/2	

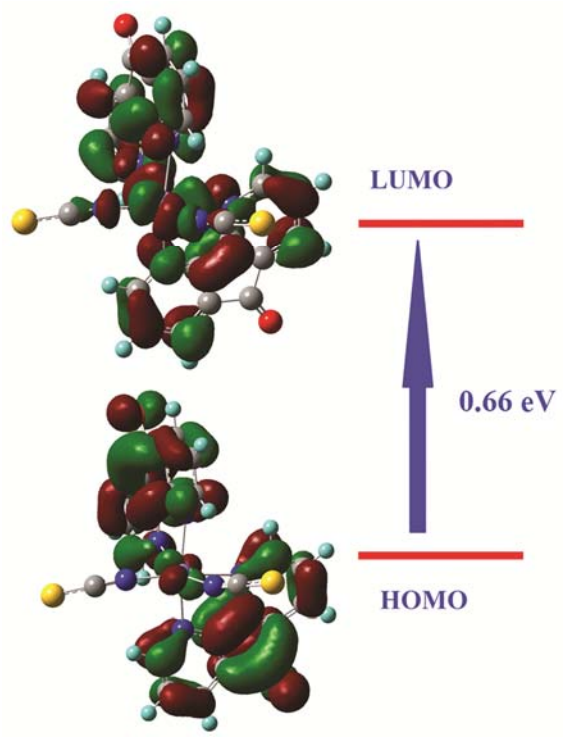

Fig. 8 — Electron distribution of the HOMO-LUMO orbitals of the $[Mn(dafone)_2(NCS)_2]$

found to be 0.0053 which indicates that the complex is soft. The electron distribution of the HOMO-LUMO orbital's of $[Mn(dafone)_2(NCS)_2]$ is given (Fig. 8).

Conclusion

Complex $[Mn(dafone)_2(NCS)_2]$ was prepared by solvent– based synthesis method using acetonitrile and methanol as solvent. Characterisation of ligand and complexes were done by elemental and various spectral analysis. The structure of the complex was confirmed by Single–crystal X-ray diffraction studies. The complex shows octahedral geometry. Cytotoxicity of the complex was studied based on percentage viability of the cell evaluated by direct observation of cells by inverted phase–contrast microscope followed by MTT assay method. The complex was found to be more active against cervical carcinoma cells than fibroblast cells in any of the metal concentrations varying from 0-100 µg/mL. Its photocatalytic activity was clear from the photodegradation plot of methylene blue dye.

Acknowledgement

CCDC deposit number for the single crystal x-ray structure is CCDC- 2039258. We thank Biogenix Research Centre, Thiruvananthapuram, Kerala, India for cytotoxic studies, SAIF STIC CUSAT, Kerala, India for the XRD analysis, Solid– state electronic spectra & CHN analysis, & National Institute for Interdisciplinary Science and Technology, Thiruvananthapuram, Kerala, India for ^{1}H NMR spectra.

Reena thank University Grants Commission for the FDP fellowship and ARB thank the FIST –UGC fund for the IR spectrophotometer at Sir Syed College, Taliparamba, Kerala.

B. Kishore babu and K.Mohana Rao acknowledge grants from the Ref No: 42-354/2013 UGC (INDIA), New Delhi. We are grateful for the technical assistance provided by the Department of Engineering Chemistry at the Andhra University, Visakhapatnam (INDIA) and the University of Hyderabad for providing the spectral data.

Conflict of interest

All authors declare no conflict of interest.

References

1 Henderson Jr LJ, Fronczek FR & Cherry WR, Selective perturbation of ligand field excited states in polypyridine ruthenium(II) complexes. *J Am Chem Soc*, 106 (1984) 5876.

2 Prasad K, Subhash P& Ekkehard S, Neutral metal complex in an ionic pocket: synthesis, physicochemical properties and X-ray structure of a copper(II) complex containing neutral as well as cationic dafone ligands and dafonium perchlorate. *Inorganica Chimica Acta*, 321 (2001) 193.

3 Lu Z, Duan C, Tian Y & You X, Synthesis, Characterization, and Crystal Structure of a Novel Copper(II) Complex with an Asymmetric Coordinated 2,2'-Bipyridine Derivative: A Model for the Associative Complex in the Ligand-Substitution Reactions of $[Cu(tren)L]^{2+}$. *Inorg Chem*, 35 (1996) 2253.

4 Treshchalina EM, Konovalova AL, Presnov MA, Chapurina LF & Belichuk NI, Antitumor properties of mixed coordination compounds of copper (II) and alpha-amino acids. *Dokl Akad Nauk (SSSR)*, 248 (1979) 1273.

5 Brown DB, Khokhar AR, Hacker MP, Lokys L, Burchenal JH, Newman RA, McCormack JJ & Frost D, Synthesis and antitumor activity of new platinum complexes. *J Med Chem*, 25 (1982) 952.

6 Saeed-ur-Rehman, Muhammad I, Sadia R, Alia F & Shahnawaz, Synthesis, characterization and antimicrobial studies of transition metal complexes of imidazole derivative. *Bull Chem Soc Ethiop*, 24 (2010) 201.

7 Mirabelli CK, Hill DT, Faucette LF, McCabe FL, Girard GR, Bryan DB, Sutton BM, Bartus JO, Crooke ST & Johnson RK, Antitumor activity of bis(diphenylphosphino)alkanes, their gold(I) coordination complexes, and related compounds. *J Med Chem*, 30 (1987) 2181.

8 Kelland LR, New platinum antitumor complexes. *Crit Rev Oncol Hematol*, 15 (1993) 191.

9 Kelland LR, Barnard CF, Mellish KJ, Jones M, Goddard PM, Valenti M, Bryant A, Murrer BA & Harrap KR, A novel

trans-platinum coordination complex possessing *in vitro* and *in vivo* antitumor activity. *Cancer Res*, 54 (1994) 5618.

10 Ganesh KN, Satya D P, Sathi M, Sudip K G, Panchanan P & Anindya S G, Thiol stabilized copper nanoparticles exert antimicrobial properties by preventing cell division in *Escherichia coli*. *Indian J Biochem Biophy*, 57 (2020) 151.

11 Swadesh S, Amrita P, Anirban C & Santanu P, A novel compound β-sitosterol-3-O-β-D-glucoside isolated from *Azadirachta indica* effectively induces apoptosis in leukemic cells by targeting G0/G1 populations. *Indian J Biochem Biophys*, 57 (2020) 27.

12 Kurbacher CM, Nagel W, Mallmann P, Kurbacher JA, Sass G, Hubner H, Andreotti PE & Krebs D, *In vitro* activity of titanocenedichloride in human renal cell carcinoma compared to conventional antineoplastic agents. *Anticancer Res*, 14 (1994) 1529.

13 Friedrich M, Villena-Heinsen C, Farnhammer C & Schmidt W, Effects of vinorelbine and titanocene dichloride on human tumour xenografts in nude mice. *Eur J Gynaecol Oncol*, 19 (1998) 333.

14 Roy S, Hagen KD, Maheswari PU, Lutz M, Spek AL, Reedijk J & Van Wezel GP, Phenanthroline derivatives with improved selectivity as DNA-targeting anticancer or antimicrobial drugs. *Chem Med Chem*, 3 (2008) 1427.

15 Marzano C, Pillei M, Tisato F & Santini C, Copper complexes as anticancer agents. *Anticancer Agents Med Chem*, 9 (2009) 185.

16 Biju AR, Rajasekharan MV, Satish S Bhat, Ayesha A Khan & Avinash S Kumbhar Synthesis, crystal structure and cytotoxicity studies of cis-dichloro(4,5-diazafluoren-9-one)platinum(II). *Inorganica Chimica Acta*, 423 (2014) 93.

17 Zhu HL, Zhang XM & Liu XY, Clear Ag-Ag bonds in three silver(I) carboxylate complexes with high cytotoxicity properties. *Inorg Chem Commun*, 6 (2003) 1113

18 Liu JJ, Galettis P, Farr A, Maharaj L, Samarasinha H, McGechan AC, Baguley BC, Bowen RJ, Berners-Price SJ & McKeage MJ, *In vitro* antitumour and hepatotoxicity profiles of Au(I) and Ag(I) bidentate pyridyl phosphine complexes and relationships to cellular uptake. *J Inorg Biochem*, 102 (2007) 303.

19 Solomon EI, Sundaram UM & Machonkin TE, Multicopper Oxidases and Oxygenases. *Chem Rev*, 96 (1996) 2563.

20 Tripathi L, Kumar P, Singhai AK, Role of chelates in treatment of cancer. *Indian J Cancer*, 44 (2007) 62.

21 Shannon MA, Bohn PW, Elimelech M, Georgiadis JG, Marinas BJ & Mayes AM, Science and technology for water purification in the coming decades. *Nature*, 452 (2008) 301.

22 Hoffmann MR, Martin ST, Choi W & Bahneman DW, Environmental applications of semiconductor photocatalysis. *Chem Rev*, 95 (1995) 69.

23 Zhiyong Y, Laub D, Bensimon M & Kiwi J, Flexible polymer TiO_2 modified film photocatalysts active in the photodegradation of azo-dyes in solution. *Inorg Chim Acta*, 361 (2008) 589.

24 Macwan DP, Dave PN & Chaturvedi S, A review on nano-TiO_2 sol–gel type syntheses and its applications. *J Mater Sci*, 46 (2011) 3669.

25 Ungelenk J & Feldmann C, Adjustable kinetics in heterogeneous photocatalysis demonstrating the relevance of electrostatic interactions. *Appl Catal B: Environ*, 127 (2012) 11.

26 Mena E, Reya A, Acedo B, Beltrán FJ & Malato S, TiO2 photocatalytic oxidation of a mixture of emerging contaminants: A kinetic study independent of radiation absorption based on the direct-indirect model. *Chem Eng J*, 204–206 (2012) 131.

27 Ge L & Liu J, Photocatalytic active Bi2WO6 sensitized by CdS quantum dots (QDs). *Appl Catal B: Environ*, 105 (2011) 289.

28 Pyle AM, Rehmann JP, Meshoyrer R, Kumar CV, Turro NJ & Barton JK, Mixed-ligand complexes of ruthenium(II): factors governing binding to DNA. *J Am Chem Soc*, 111 (1989) 3051.

29 Kumari NKP & Jagannadham MV, Organic solvent induced refolding of acid denatured heynein: molten: Evidence of domains in the molecular structure of the protein and their sequential unfolding. *J Protein Proteomics*, 2 (2011) 11.

30 Prasanna Kumari NK & Jagannadham, MV, Deciphering the molecular structure of cryptolepain in organic solvents. Biochimie, 94 (2012) 354.

31 Menon S, Balagopalakrishna C, Rajasekharan MV & Ramakrishna BL, Synthesis, Crystal Structure, Magnetic Susceptibility, and Single-Crystal EPR Studies of $[DafoneH_2][(CuCl_3H_2O)Cl]$. *Inorg Chem*, 33 (1994) 950.

32 Menon S & Rajasekharan MV, A Channel-Forming Polyiodide Network in $[Cu(dafone)_3]I_{12}$. A Tris Chelate of Dafone and a New Planar Structure for the I_{12}^{2-} Ion (Dafone = 4,5-Diazafluoren-9-one). *Inorg Chem*, 36 (1997) 4983.

33 Menon S & Rajasekharan MV, Bis chelate Cu(II) complexes of dafone—synthesis, structural, EPR and optical spectral studies. *Polyhedron*, 17 (1998) 2463.

34 Miao S, Kang H, Du C & Ji B, Nickel complexes of 4, 5-Diazafluoren-9-one. *X-Ray Struct Anal Online*, 22 (2006) 45.

35 Wu ZY & Xu DJ, cis-Dichlorobis(4,5-diazafluoren-9-one-K^2N,N')manganese(II) ethanol Solvate. *Acta Cryst E*, 60 (2004) m839.

36 Shi XU, You XZ, Li C & Xiong RG, *Trans Met Chem*, 20 (1995) 191.

37 Maguire L, Seward CM, Baljak S, Reumann T, Ortin Y, Banide E & Nikitin K, Muller-Bunz H, McGlinchey MJ. *Eur J Inorg Chem*, (2009) 3250.

38 Barbara M, Mariusz W, Joanna P, Anna S, Nawrot I & MichalikKrishna K, Cu(II), Ni(II) and Hg(II) thiocyanate complexes incorporating 4,5-diazafluoren-9-one: Synthesis spectroscopic characterization X-ray studies & magnetic properties. *Struct Chem*, 22 (2011) 1053.

39 Kishore BB, Elahi SM, Krishna CT & Rajasekharan, Synthesis and Structural Studies of copper(II) and nickel(II) complexes containing 4,5-diazafluoren-9-one and pseudohalides: Metal ion directed isomer preference. *Indian J Chem*, 50A (2011) 1318.

40 Tabbi G, Fry SC & Bonomo RP, ESR study of the non-enzymic scission of xyloglucan by an ascorbate-H_2O_2-copper system: the involvement of the hydroxyl radical and the degradation of ascorbate. *J Inorg Biochem*, 84 (2001) 179.

41 Verma P, Baldrian P & Nerud F, Decolorization of structurally different synthetic dyes using cobalt (II)/ascorbic acid/hydrogen peroxide system. *Chemosphere*, 50 (2003) 975.

42 Bruker SAINT, XPREP, APEX2 and SADABS. (Bruker AXS Inc, Madison, Wisconsin, USA) (2004).

43 Altomare A, Cascarano G, Giacovazzo C, Guagliardi A, Burla MC, Polidori G & Camalli M, SIR92 - a program for

automatic solution of crystal structures by direct methods. *J Appl Cryst*, 27 (1994) 435.

44 Sheldrick GM, Crystal structure refinement with *SHELXL*. *Acta Cryst C*, 71 (2015) 3.

45 Macrae CF, Edgington PR, McCabe P, Pidcock E, Shields GP, Taylor R, Towler M & Van de Streek J, Mercury: Visualization and Analysis of Crystal Structures. *J Appl Cryst*, 39 (2006) 453.

46 Westrip SP, publCIF: software for editing, validating and formatting crystallographic information files. *J Appl Cryst*, 43 (2010) 920.

47 Frisch MJ, Trucks GW, Schlegel HB, Scuseria GE, Robb MA, Cheeseman JR, Scalmani G, Barone V, Mennucci B, Petersson GA, Nakatsuji H, Caricato M, Li X, Hratchian HP, Izmaylov AF, Bloino J, Zheng G, Sonnenberg JL, Hada M, Ehara M, Toyota K, Fukuda R, Hasegawa J, Ishida M, Nakajima T, Honda Y, Kitao O, Nakai H, Vreven T, Montgomery JA, Jr Peralta JE, Ogliaro F, Bearpark M, Heyd JJ, Brothers E, Kudin KN, Staroverov VN, Kobayashi R, Normand J, Raghavachari K, Rendell A, Burant JC, Iyengar SS, Tomasi J, Cossi M, Rega N, Millam JM, Klene M, Knox JE, Cross JB, Bakken V, Adamo C, Jaramillo J, Gomperts R, Stratmann RE, Yazyev O, Austin AJ, Cammi R, Pomelli C, Ochterski JW, Martin RL, Morokuma K, Zakrzewski VG, Voth GA, Salvador P, Dannenberg JJ, Dapprich S, Daniels AD, Farkas Ö, Foresman JB, Ortiz JV, Cioslowski J, Fox DJ, Gaussian 09, Revision E.01.(Gaussian, Inc., Wallingford CT) (2009).

48 Becke AD, A new mixing of Hartree-Fock and local density-functional theories. *J Chem Phys*, 98 (1993) 1372.

49 Geary WJ, The Use of Conductivity Measurements in Organic Solvents for the Characterisation of Coordination Compounds. *Coord Chem Rev*, 7 (1971) 81.